16TH EUROPEAN CONFERENCE ON EARTHQUAKE ENGINEERING THESSALONIKI 18 - 21 JUNE 2018

DEVELOPMENT OF FRAGILITY CURVES FOR USE IN SEISMIC RISK TARGETING

Athanasios GKIMPRIXIS[1], John DOUGLAS[2], Enrico TUBALDI[3], Daniele ZONTA[4]

ABSTRACT

Many studies have shown that designing structures in a region by applying the 'uniform hazard' principle does not guarantee that the risk of collapse throughout this region will also be uniform. In other words, using constant-return-period ground motions for design leads to structures exposed to different levels of earthquake risk, even though they are designed according to the same regulations. Recently, a more sophisticated approach, often referred to as 'risk-targeting', has been developed and applied in practice in the US, while studies have also been conducted for France, Romania and Indonesia, as well as for the whole of Europe.
In this study, we design, based on Eurocodes 2 and 8, a set of six reinforced concrete buildings corresponding to different geometries and two levels of design peak ground acceleration (0.1 and 0.3g). The response of these buildings to earthquake shaking is modelled numerically using state-of-the-art computer software to develop fragility curves for different limit states. We find that while the design acceleration has some influence on the fragility curves, other parameters such as the number of storeys also affect them. These preliminary results are useful for improving the procedures for risk-targeting.

Keywords: risk targeting; seismic design; fragility curves; vulnerability; reinforced concrete

1. INTRODUCTION

A key input when designing a new structure using Eurocode (EC) 8 (CEN 2004), the European seismic design code, is the design acceleration (a_g). This acceleration is used to construct the design response spectrum, which also depends on the site class (A, B, C, etc.). The general aim of EC8 is that the higher the a_g, the more resistant to earthquake shaking is the designed structure. In this study we conduct a preliminary investigation of the impact of a_g on the vulnerability of reinforced-concrete (RC) structures designed using Eurocodes 2 and 8. The purpose of this investigation is to improve our understanding of whether a_g dominates over other factors affecting vulnerability, in our case the number of storeys and number of bays. The ultimate aim of our research project is to develop fragility curves that could be used within a risk-targeting approach for seismic design (Luco et al., 2007).
In this section a brief introduction to the approach of risk-targeting for the development of seismic design maps is provided alongside a summary of previous studies providing the critical input to this approach that is further investigated here, i.e.: fragility curves for different design accelerations. Section 2 presents the structures that we have designed using EC2 and EC8 for our study. Next the procedure used to construct the fragility curves of those structures is presented. In Section 4 the results of these calculations are shown and compared to curves derived in previous studies. The article ends with some brief conclusions and recommendations for future work.

[1]PhD student, University of Strathclyde, Glasgow, UK, athanasios.gkimprixis@strath.ac.uk
[2]Dr, University of Strathclyde, Glasgow, UK, john.douglas@strath.ac.uk
[3]Dr, University of Strathclyde, Glasgow, UK, enrico.tubaldi@strath.ac.uk
[4]Prof, University of Strathclyde, Glasgow, UK, daniele.zonta@strath.ac.uk

1.1 Risk-targeting

In the approach for the development of seismic design maps commonly known as risk-targeting, rather than mapping the design acceleration from a probabilistic seismic hazard assessment (PSHA) for a constant return period (e.g. 475 years), the design accelerations that lead to a constant level of risk of collapse (or other damage level) are mapped. To calculate these accelerations an iterative approach is required where, for each location, the hazard curve from the PSHA is convolved with a fragility curve expressing the probability of collapse given an acceleration to evaluate the annual probability of collapse for a structure designed to that standard. The iteration continues until this probability of collapse equals the chance of collapse that is considered acceptable. The interested reader is referred to Douglas et al. (2013) for a detailed discussion of this approach and an application for France.

Risk-targeting has three principal advantages over the use of design levels that are defined in the traditional 'uniform hazard' way, i.e. for a given return period (e.g. 475 years). These advantages are (Douglas and Gkimprixis, 2018): transparency, a risk level that is uniform across a territory and the ability to compare (and ideally control) risk for different types of hazard (e.g. earthquake versus wind). It does, however, come with the disadvantage of making more choices explicit, rather than implicitly being assumed through convention (e.g. the choice of 475 years as the design return period).

1.2 Previous studies presenting fragility curves for code-designed structures

As discussed above, in a risk-targeting approach, seismic risk is calculated by convolving the seismic hazard curve of a given location with a fragility curve for a code-designed structure (ideally derived from structural modelling). The ground-motion level that the structure is designed for is chosen so that the structure has a pre-defined probability of achieving a certain performance level (e.g. non-collapse). Determining fragility curves for structures designed with modern codes for different levels of ground motion is, therefore, a prerequisite for the application of the method. In this section, we briefly summarize previous studies proposing fragility curves for code-designed structures for different levels of design acceleration. Only studies that have derived fragility curves for two or more levels of design acceleration are summarized here. This is because the large dispersion between fragility curves from different studies makes drawing conclusions on the effect of design accelerations on the vulnerability of the structure difficult. For example, if one study presents a fragility curve for a 3-storey RC building designed for a 0.1g peak ground acceleration (PGA) and another study presents a curve for a comparable building but designed for 0.3g, the differences could be due to the design acceleration or they could be due to (minor) differences in the design approach or fragility curve derivation (e.g. selected strong-motion records, damage thresholds and fitting technique).

In a previous study, Ulrich et al. (2014) developed fragility curves in terms of PGA for EC8-designed RC structures but only for a single building geometry (3 storey-3 bay) and a handful of design accelerations: 0.0 (gravity loads only), 0.7, 1.1, 1.7, 2.3 and 3.0 m/s^2. One of the conclusions reached was that the fragility curves for design accelerations of 1.1 m/s^2 (0.11g) or lower were similar and overall the impact of the design acceleration on the vulnerability was quite low. This suggests that using code design procedures even without considering earthquake loading leads to robust structures and the correlation between design acceleration and earthquake vulnerability is weak.

Martins et al. (2015) consider 3-storey and 5-storey RC 3-bay-4-frames structures designed for 0.0, 0.2 and 0.4g. They present the fragility curves for these six structures both in terms of spectral acceleration and PGA. One observation that can be made from the presented curves is that the effect of the number of storeys on the fragility curves derived for the same design accelerations is high. The curves of Martins et al. (2015) show a higher effect of the design acceleration on the vulnerability of the structures than the curves of Ulrich et al. (2014).

2. DESIGN OF STRUCTURES USING EUROCODE 8

In this section the approach for the design of the structures and their characteristics are presented.

2.1 Structures considered

The modelled structures are standard RC buildings (Importance class II), which are symmetrical in plan and elevation. The buildings are chosen so that the influence of the design acceleration, the number of bays and the number of storeys on the fragility curves can be investigated. In particular, 2-storey-2-bay buildings are designed for two design PGAs (a_g): 1m/s^2 (0.1g) and 3m/s^2 (0.3g) and 4-storey-2-bay and 2-storey-4-bay buildings for the same design PGAs are considered as well. A medium ductility class is assumed for all models. The buildings are square in plan, with bay lengths of 5m. The length of the columns is also constant and equal to 3m. The material properties, which are the same for all the models, are presented in Table 1.

Table 1. Properties of concrete and steel used in modelled structures.

Concrete		**Steel**	
Characteristic strength (kPa)	25,000	Characteristic strength (kPa)	450,000
Mean compressive strength (kPa)	33,000	Mean strength (kPa)	517,500
Mean tensile strength (kPa)	2,600	Modulus of elasticity (kPa)	$2.00 \cdot 10^8$
Modulus of elasticity (kPa)	$3.10 \cdot 10^7$	Strain hardening parameter (-)	0.005
		Fracture/buckling strain (-)	0.106

2.2 Design approach

The considered structures are all designed to be compliant with the EC2 and EC8 regulations. Since the models are regular both in plan and elevation, the codes allow the use of a simplified 2D design and modelling approach. To be conservative, an internal frame is considered, by neglecting torsional effects.

The finite element software SAP2000 is used to design the structures following EC2 and EC8. The simplified approach of EC8-1-4.3.1(7) is implemented to take into account the effect of cracking. To this end, a 50% reduction of the materials' modulus of elasticity is considered for the elements of all the models. For the structural design, the characteristic values of Table 1 are used for the concrete and steel properties. A value of 25 KN/m^3 was assumed for the specific weight of reinforced concrete. The assumptions of fixity at base and of rigid diaphragms in each storey are also made. The contribution of the slab (15 mm thick) to the lateral stiffness was considered by assuming T-shaped beams, an approach compliant with the codes. For more information on this point, the reader is referred to EC2-1.1-5.3.2.1, which deals with the estimation of the effective beam width (b_{eff}).

The first step of the design procedure is to define some minimum dimensions for the sections. It is noted that both the columns and the beams have the same section for all storeys. The models are analysed both for gravitational and earthquake loading. Regarding the permanent load, 1KN/m^2 was assumed for the finishing weight and 1.5 KN/m^2 and 3.25 KN/m^2 for the internal and external walls of the intermediate storeys, respectively. In the perimeter of the roof, a load of 3.75 KN/m was assumed instead. The distributed live load (Q) was taken equal to 2 KN/m^2 and 2.5 KN/m^2 for the roof and intermediate storeys, respectively.

The following two load combinations are considered for the design: 1.35·G+1.5·Q and G+0.3·Q+E, where G, Q and E are the permanent, live and earthquake loads respectively. It is highlighted that the first load combination (gravity loads only) needs to be checked, since it could control the section dimensions and reinforcement for low design acceleration values. Assuming soil class B conditions and 5% for the damping ratio, the EC8 Type 1 horizontal design acceleration spectrum is calculated. A behaviour factor q = 3.9 is considered (EC8-1-5.2.2.2), to define the design spectrum. The earthquake forces are calculated and applied to the model based on the mass distribution, following the lateral force method described in EC8-1-4.3.3.2.

The required reinforcement area (longitudinal and shear) for beams and columns is then calculated, according to the requirements of the codes. An additional check is made manually according to EC8-1-4.4.2.2(2) regarding the second-order effects. The limitation of interstorey drift (maximum 0.5% storey drift) is also checked, in accordance with the criterion of paragraph EC8-1-4.4.3.2, by employing a value of 0.5 for the reduction factor v. The beneficial contribution of the infills in terms

of added stiffness and strength for low seismic intensities is disregarded.
If the structure fails any of the above criteria, the sections are increased by the user. Otherwise, the design procedure is complete and the resulting maximum values are considered for simplicity. The results of this procedure are summarized in Table 2. Our calculated dimensions are comparable with those presented by Fardis et al. (2012) for similar structures designed using EC2 and EC8.

Table 2. Properties of the designed structures.

Model		Beams					Columns		First modal period (s)
storeys-bays-design PGA(m/s^2)	Storey	H (cm)	W (cm)	beff (m)	Top reinf. (mm)	Bottom reinf. (mm)	H=W (cm)	Reinf. (mm)	
2-2-1	1	30	25	1.65	2Φ24	2Φ16	35	4Φ20	0.37
	2	30	25	1.65	2Φ18+3Φ14	4Φ12			
2-2-3	1	35	30	1.70	4Φ20	3Φ16	40	8Φ16	0.28
	2	35	30	1.70	2Φ24	2Φ16			
2-4-1	1	25	25	1.65	3Φ22	2Φ18	35	8Φ14	0.40
	2	25	25	1.65	2Φ24	2Φ16			
2-4-3	1	35	30	1.70	5Φ18	5Φ12	40	4Φ24	0.29
	2	35	30	1.70	3Φ18	3Φ12			
4-2-1	1	30	25	1.65	3Φ20	2Φ16	35	8Φ14	0.76
	2	30	25	1.65	2Φ24	2Φ16			
	3	30	25	1.65	4Φ16	2Φ16			
	4	30	25	1.65	4Φ14	3Φ12			
4-2-3	1	50	45	1.85	7Φ18	6Φ16	50	8Φ20	0.38
	2	50	45	1.85	2Φ22+2Φ24	4Φ18			
	3	50	45	1.85	3Φ18+2Φ16	3Φ16			
	4	50	45	1.85	3Φ16	3Φ16			

3. CONSTRUCTION OF FRAGILITY CURVES

In this section, the method used to model numerically the code-design structures is discussed.

3.1 Dynamic modelling

The finite element software Seismostruct is used for performing the seismic analyses. The software uses the fibre approach to distribute plasticity across an element's section. In our case, 150 fibres are employed, based on accuracy and computational efficiency criteria. A forced-based formulation is used to model the elements and the plastic-hinge method is employed to distribute plasticity across the elements' length (Calabrese et al., 2010). The length of the plastic hinge (L_p) is calculated according to the Paulay and Priestley (1992) formula:

$$L_p = 0.08 \cdot L + 0.022 \cdot f_y \cdot d_b \quad (1)$$

where L is the element's length and f_y and d_b the yield strength and diameter, respectively, of the longitudinal reinforcing steel.
Regarding the material properties, the Kappos and Konstantinidis (1999) nonlinear concrete model was used alongside a steel model based on Menegotto and Pinto (1973). In the design approach described in the former section, the characteristic values were used. However, for the performance of nonlinear analyses, the mean values of Table 1 are used instead, as stated in EC8-1-4.3.3.4.1(4). Once again, we should highlight that the masonry infills were not considered in the nonlinear modelling.
A Rayleigh damping matrix, built based on the tangent stiffness approach, is employed to model the damping inherent to the structure and its contribution to the seismic energy dissipation. A 5% damping

ratio is considered for the first two transitional modal periods (estimated via eigenvalue analysis). Finally, the seismic combination includes both the permanent loads (G+0.3·Q, where G denotes the permanent loads and Q the live ones) and the seismic excitation (acceleration in the horizontal direction) at the base nodes.

3.2 Strong-motion records

The structures modelled in this study are assumed to be located in a high seismicity area in the Mediterranean region, where near-source moderate and large crustal earthquakes are possible (e.g. central Italy or Greece), but not at a specific site. A set of strong-motion records reflecting the earthquake shaking that the structures could be subjected to was selected from RESORCE (Akkar et al., 2014) using these selection criteria: epicentral distance between 0 and 30km, moment magnitude between 5 and 7 and focal depth less than or equal to 30km. 25 records, with unscaled peak ground accelerations (PGA) from 2.1m/s^2 to 8.7m/s^2, were selected. For the calculation of the fragility curves the records were all scaled to a set of 26 roughly logarithmically-spaced PGAs between 0.15m/s^2 and 60m/s^2. The linear elastic response spectra for 5% critical damping of the 25 records scaled to a common PGA of 5m/s^2 are shown in Figure 1, along with the average spectrum and the first modal periods of the designed structures.

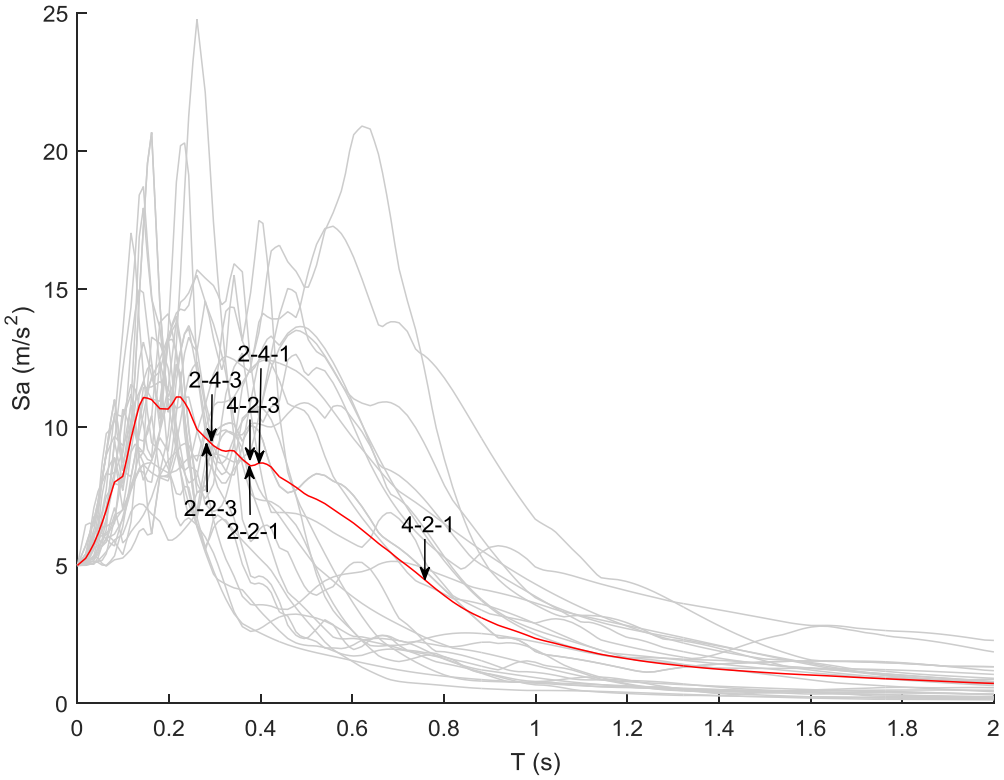

Figure 1: Linear elastic response spectra (5% damping) of the 25 selected strong-motion records scaled to a common PGA of 5m/s^2 (grey), the average spectrum (red) and the first modal periods of the designed structures.

3.3 Fitting of fragility curves

Nonlinear time history analyses were performed with the selected records. As stated above, for each model the 25 selected records were scaled at 26 different intensity levels and used as input. From the results of the analyses, the maximum interstorey drift was selected for each PGA level, thus creating a cloud of 25 × 26= 650 points, for each model.

Similar to Ulrich et al. (2014), two limit states are considered in this study, namely the 'no damage' and 'severe damage' of Ghobarah (2004). The first limit state corresponds to some fine cracks forming

in plaster, whereas the second corresponds to partial collapse of lateral and gravity load carrying elements. These limit states are controlled by the interstorey drift ratios limits, equal to 0.2% and 1.8% respectively for the 'no damage' and 'severe damage' limit state, as suggested in Ghobarah (2004). The limit state of 'light damage', with a 0.4% threshold (Ghobarah 2004), is also examined since it is regarded by the authors to be more representative of the yield scenario (compared to the conservative 0.2%).

When estimating the response of structures to extreme ground motions, it is common that the numerical simulations do not converge. Therefore, particularly for the 'severe damage' level, it is not possible to obtain accurate drift estimates for all strong-motion records scaled to high PGAs. In this situation, the standard least-squares (LS) regression on a cloud cannot be used and the maximum-likelihood estimation (MLE) (Shinozuka et al., 2000) is preferable (e.g. Gehl et al., 2015). This is despite the higher uncertainties in the derived fragility curves for the same number of dynamic runs using MLE as opposed to LS regression (Gehl et al., 2015). The likelihood function method requires only knowledge of whether the monitored limit state has been exceeded or not for the strong-motion record considered. We assume that simulations that do not converge indicate that the structure has collapsed, which is a common assumption.

For consistency, results for every limit state are derived using the MLE method assuming a lognormal fragility curve with two free parameters: the median capacity, α, and the standard deviation, β. Comparisons between fragility curves derived using MLE and LS regression for 'no damage' limit state have been carried out, and the observed differences are minimal.

The following equation describes the probability of being at or exceeding a particular damage state (ds_i) for a given intensity ($IM=im$):

$$P(ds \geq ds_i | IM = im) = \Phi\left[\frac{ln(x/\alpha)}{\beta}\right] \quad (2)$$

where Φ is the cumulative distribution function of the standard normal distribution. This equation is used to fit the output of the dynamic analyses.

4. RESULTS

Figure 2 presents the fragility curves of the case study for the damage states of 'light damage' and 'severe damage'. The coefficients of the lognormal fragility curves according to Equation 2 are given in Table 3. In general, it is observed that by increasing the design PGA, the median capacity of the building increases. Moreover, the 2-storey and 4-storey buildings designed for the same PGAs are characterized by different vulnerabilities. In particular, the 4-storey buildings experience lower interstorey drift demands and hence are less vulnerable than the 2-storey ones. The same trend can be observed in the works of Tsionis and Fardis (2014) and Fardis et al. (2012), although this is not seen in the results of Martins et al. (2015). The difference between the fragility curves of the 2- and 4-storey buildings is larger for higher design PGA values. This can possibly be attributed to the clause of the codes that controls the interstorey drifts at the damage limitation limit state, which results in a conservative design (i.e. sections with large dimensions) for the 4-2-3 model. The standard deviation, β, of the fragility curves, another critical parameter in the risk-targeting approach, shows consistent values with an average of 0.65 for the case of 'severe damage' (Table 3), which is close to the 0.6 proposed in ASCE 7-10. It should be noted that the obtained results could be affected also by the records selected to describe record-to-record variability effects (Figure 1).

The results shown in Figure 2 and Table 3 also allow an evaluation of the influence of the geometry (in terms of number of bays only) on the fragility curves. It can be observed that the number of bays has a minor impact on these curves. This is expected, since if the span dimensions are kept constant, while the stiffness changes, so does the total mass, resulting in minor changes in the dynamic behaviour of the structure. This last point can also be seen by comparing the modal periods of the structures (see Table 2).

Table 3. Coefficients of the fragility curves.

Model	No damage		Light Damage		Partial Collapse	
	α	β	α	β	α	β
2-2-1	0.953	0.504	1.784	0.549	8.627	0.638
2-2-3	1.099	0.447	2.282	0.490	9.175	0.688
2-4-1	0.934	0.518	1.668	0.591	8.150	0.622
2-4-3	1.253	0.440	2.281	0.476	9.234	0.699
4-2-1	1.032	0.486	2.220	0.518	10.272	0.659
4-2-3	1.613	0.568	2.814	0.621	11.951	0.604

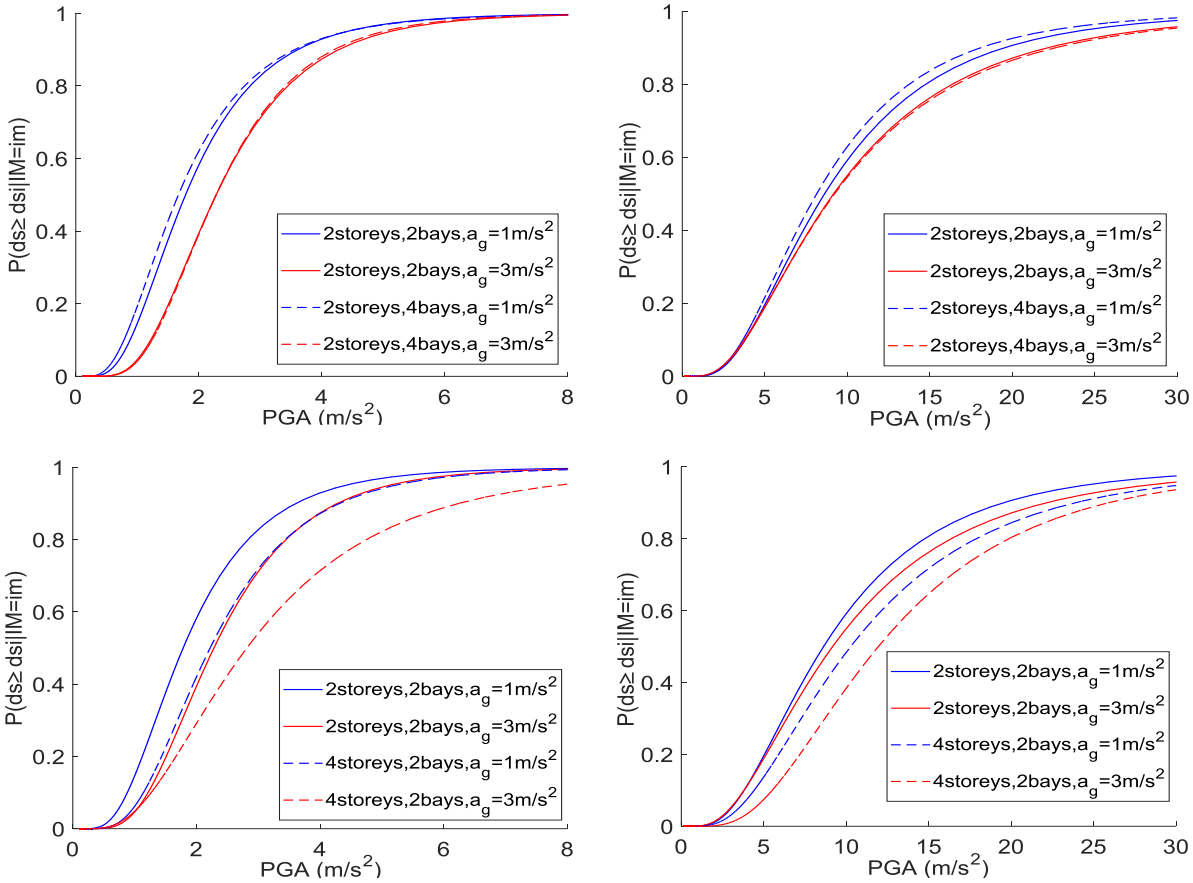

Figure 2: Influence of the number of bays (top figures) and storeys (bottom figures) on the fragility curves, for the 'light damage' (left) and 'severe damage' (right) limit states.

Table 4 reports the probability of experiencing different damage levels at the design PGA obtained from the derived fragility curves. The probability of 'severe damage' when exposed to a PGA level equal to the design value is a necessary input when implementing the current risk-targeting approach (e.g. Douglas et al., 2013), although the approach could be modified to use fragility curves anchored to any PGA level. For the case study investigated here and under the assumptions discussed before, this probability is in the range 10^{-4} to 10^{-2} when designing for 0.1g and 0.3g, respectively. These values are higher than the ones presented in Ulrich et al. (2014) for their case study.

Table 4. Probabilities of different levels of damage at the design PGA.

Model	No damage	Light Damage	Severe Damage
2-2-1	0.538	0.146	$3.63 \cdot 10^{-4}$
2-2-3	0.988	0.712	$5.20 \cdot 10^{-2}$
2-4-1	0.552	0.193	$3.71 \cdot 10^{-4}$
2-4-3	0.976	0.718	$5.39 \cdot 10^{-2}$
4-2-1	0.474	0.062	$2.02 \cdot 10^{-4}$
4-2-3	0.863	0.541	$1.10 \cdot 10^{-2}$

As for the 'no damage' limit state, the average values are equal to 0.521 for 0.1g and 0.942 for 0.3g, quite close to the ones presented in Ulrich et al. (2014) for their yield damage state, which corresponds to the same interstorey drift ratio limit of 0.2% as the one considered here. For 'light damage', an average value of 0.134 is observed for 0.1g and 0.657 for 0.3g. The general trend is similar to the results of Martins et al. (2015).

5. CONCLUSIONS

This study is a first step towards defining fragility curves that are useful for risk-targeting, which is a design philosophy currently attracting considerable research effort. The impact of the design acceleration and the number of bays and storeys on the probability of occurrence of different limit states is investigated herein. In subsequent work we plan to investigate the influence of the strong-motion records selection and the choice of the damage state limits because these may have a significant impact on the derived fragility curves.

Some codes (e.g. ASCE) already use the risk-targeting approach and employ a simplified approach, by assuming a-priori values for the dispersion of the fragility curve (β=0.6) as well as for the probability of failure at the design PGA. The study results show that while the assumption of a constant β is realistic for the types of buildings investigated, the other assumption of a fixed probability of failure at the design PGA appears too strong. The buildings designed for 0.1g and 0.3g have probabilities of 'severe damage' roughly between 10^{-4} and 10^{-2}, i.e. with two orders of magnitude difference. Thus, future studies should investigate the effect of the assumption of a constant probability of failure at the design PGA on the final design results. The error in the risk estimates resulting from the use of the simplifying assumption when defining generic fragility curves should be evaluated by performing extensive parametric analyses for different building and hazard scenarios and by comparing the results obtained using analytical fragility curves like those developed in this study.

6. ACKNOWLEDGMENTS

We thank Thomas Ulrich for helping us reproduce the results of Ulrich et al. (2014).

7. REFERENCES

Akkar S, Sandikkaya MA, Senyurt M, Azari Sisi A, Ay BÖ, Traversa P, Douglas J, Cotton F, Luzi L, Hernandez B, Godey S (2014). Reference database for seismic ground-motion in Europe (RESORCE), *Bulletin of Earthquake Engineering*, 12(1): 311-339, doi: 10.1007/s10518-013-9506-8.

ASCE (2010). Minimum Design Loads for Buildings and Other Structures, ASCE Standard 7-10. *American Society of Civil Engineers*, Reston, VA.

Calabrese A, João PA, Pinho R (2010). Numerical Issues in Distributed Inelasticity Modeling of RC Frame Elements for Seismic Analysis, *Journal of Earthquake Engineering*, 14(S1): 38–68, doi: 10.1080/13632461003651869.

CEN (2004) EN 1992-1-1:2004 Eurocode 2: Design of concrete structures - Part 1-1: General rules and rules for buildings, *European Committee for Standardization*, Brussels.

CEN (2004) EN 1998-1:2004 Eurocode 8: Design of structures for earthquake resistance - Part 1: General rules, seismic actions and rules for buildings, *European Committee for Standardization*, Brussels.

Computers & Structures, Inc. (2016). SAP2000, Integrated Solution for Structural Analysis and Design, Version 19.0.0, USA.

Douglas J, Gkimprixis A (2018). Risk targeting in seismic design codes: The state of the art, outstanding issues and possible paths forward, *Seismic Hazard and Risk Assessment - Updated Overview with Emphasis on Romania*, R. Vacareanu and C. Ionescu (eds), Springer.

Douglas J, Ulrich T, Negulescu C (2013). Risk-targeted seismic design maps for mainland France. *Natural Hazards*, 65: 1999-2013, doi: 10.1007/s11069-012-0460-6.

Fardis MN, Papailia A, Tsionis G (2012). Seismic fragility of RC framed and wall-frame buildings designed to the EN-Eurocodes, *Bulletin of Earthquake Engineering*, 10: 1767–1793.

Gehl P, Douglas J, Seyedi D (2015). Influence of the number of dynamic analyses on the accuracy of structural response estimates, *Earthquake Spectra*, 31(1): 97-113, doi: 10.1193/102912EQS320M.

Ghobarah A (2004). On drift limits associated with different damage levels, *Proceedings of international workshop on performance-based seismic design concepts and implementation*, June 28th–July 1st, 2004, Bled, Slovenia.

Kappos A, Konstantinidis D (1999). Statistical analysis of confined high strength concrete, *Materials and Structures*, 32: 734-748.

Luco N, Ellingwood BR, Hamburger RO, Hooper JD, Kimball JK, Kircher CA (2007). Risk-targeted versus current seismic design maps for the conterminous United States, *SEAOC 2007 convention proceedings*, 26-29 September, Squaw Creek, USA.

Martins L, Silva V, Crowley H, Bazzurro P, Marques M (2015). Investigation of structural fragility for risk-targeted hazard assessment. *Proceedings of 12th International Conference on Applications of Statistics and Probability in Civil Engineering (ICASP12)*, 12-15 July, Vancouver, Canada.

Menegotto M, Pinto PE (1973). Method of analysis for cyclically loaded R.C. plane frames including changes in geometry and non-elastic behaviour of elements under combined normal force and bending, *Symposium on the Resistance and Ultimate Deformability of Structures Acted on by Well Defined Repeated Loads, International Association for Bridge and Structural Engineering*, Zurich, Switzerland, 15-22.

Paulay T, Priestley MJN (1992). Seismic design of reinforced concrete and masonry buildings, *John Wiley & Sons*, New York.

Seismosoft (2016). SeismoStruct - A computer program for static and dynamic nonlinear analysis of framed structures. Available from URL: www.seismosoft.com.

Shinozuka M, Feng Q, Lee J, Naganuma, T (2000). Statistical analysis of fragility curves, *Journal of Engineering Mechanics*, 126: 1224–1231.

Tsionis G, Fardis MN (2014). Seismic fragility curves for reinforced concrete buildings and bridges in Thessaloniki, *Second European Conference on Earthquake Engineering and Seismology*, 25-29 August, 2014, Turkey.

Ulrich T, Negulescu C, Douglas J (2014). Fragility curves for risk-targeted seismic design maps. *Bulletin of Earthquake Engineering*, 12(4): 1479-1491, doi: 10.1007/s10518-013-9572-y.